Philosophical Magazine

ISSN: 1478-6435 (Print) 1478-6443 (Online) Journal homepage: https://www.tandfonline.com/loi/tphm20

Deformation twinning in boron carbide particles within nanostructured Al 5083/B_4C metal matrix composites

Y. Li , Y.H. Zhao , W. Liu , Z.H. Zhang , R.G. Vogt , E.J. Lavernia & J.M. Schoenung

To cite this article: Y. Li , Y.H. Zhao , W. Liu , Z.H. Zhang , R.G. Vogt , E.J. Lavernia & J.M. Schoenung (2010) Deformation twinning in boron carbide particles within nanostructured Al 5083/B_4C metal matrix composites, Philosophical Magazine, 90:6, 783-792, DOI: 10.1080/14786430903246338

To link to this article: https://doi.org/10.1080/14786430903246338

Philosophical Magazine
Vol. 90, No. 6, 28 February 2010, 783–792

Taylor & Francis
Taylor & Francis Group

Deformation twinning in boron carbide particles within nanostructured Al 5083/B_4C metal matrix composites

Y. Li, Y.H. Zhao, W. Liu, Z.H. Zhang, R.G. Vogt, E.J. Lavernia and J.M. Schoenung*

Department of Chemical Engineering and Materials Science, University of California, Davis, CA 95616, USA

(*Received 17 June 2009; final version received 7 August 2009*)

The presence of deformation twins is documented in boron carbide reinforcement particles within a nanostructured Al 5083/B_4C metal matrix composite. High resolution transmission electron microscopy analysis suggests that these are (0001) twins. This work discusses the mechanisms responsible for their formation based on crystallographic analysis and mechanical loading conditions. Specifically, we propose that there are two potential models that can be used to describe twin formation in boron carbide particles. The structural models involve slip in the $1/3[\bar{1}100]$ $(01\bar{1}0)$ or $1/3[01\bar{1}0]$ $(01\bar{1}0)$ planes of C–C–C chains and the appropriate reconfiguration of B–C bonds. Analysis of the loading conditions experienced by the boron carbide particles indicates that local high stress intensity and the presence of a high shear force around the boron carbide particles are two factors that contribute to twin formation.

Keywords: microstructural characterization; nanostructured materials; TEM

1. Introduction

The compound boron carbide (B_4C) is of considerable interest as a monolithic material for a variety of applications including high-temperature semiconductors [1–3], and ballistic-resistant armor [4], primarily as a result of its remarkable combination of physical and thermal properties. For example, boron carbide is characterized by high temperature stability (melting temperature ~2600 K), high mechanical hardness (Vickers hardness, 3.7 GPa), and high electrical conductivity (140 S/m). Additional attributes make boron carbide a material of choice as the ceramic reinforcement in metal matrix composites [5]: it ranks third in hardness, just after diamond and cubic boron nitride, and possesses a low density of 2.51 g/cm^3 (which is even less than that of Al, 2.75 g/cm^3) [6]. The structure of boron carbide is also unusual with distinctive chemical bonding (the three carbon atoms are directly linked as C–C–C chains). This solid nominally has a rhombohedral (D^5_{3d}-$R\bar{3}m$) crystal structure [2]. The building blocks of this structure are 12-atom-deformed

*Corresponding author. Email: jmschoenung@ucdavis.edu

ISSN 1478–6435 print/ISSN 1478–6443 online

DOI: 10.1080/14786430903246338
http://www.informaworld.com

icosahedra units and the three-atom chains; the icosahedra are linked both by direct bonds and through the carbon chains.

In contrast to metals, in which defects such as dislocations critically influence mechanical behavior, the presence of dislocations or twins are generally believed to have very limited influence on the mechanical behavior of ceramics. However, some physical properties, such as optical transparency and electrical conductivity, are strongly dependent on the type and population of defects present in ceramics [7]. Not surprisingly, understanding the mechanisms that govern introduction of defects in ceramics has been the topic of numerous studies [8–11]. For example, it has been reported that dislocations and twinning of alumina can be activated during abrasion [8], and that twinning in alumina can arise during compression at elevated temperatures [10]. In related studies, the mechanism responsible for the formation of twins in alumina is described in detail [11–13]. In comparison to studies of the defect structures present in alumina, the defect structures that are present in boron carbide have received only limited attention. For example, Jostsons and co-workers [9,14,15] document the presence of dislocations in boron carbide. In related work, Tamburini and co-workers [14,16,17] report the presence of twins in boron carbide, and proposed a model on the basis of XRD analysis. However, inspection of the published literature shows that a detailed crystallographic model of twin formation in boron carbide has not been proposed and, moreover, reports of twinning in a metal matrix composite reinforced with boron carbide have heretofore never been documented.

In this paper, we report the presence of deformation twins in boron carbide reinforcement particles within a nanostructured Al 5083/B_4C metal matrix composite. The twin structure was studied with detailed high-resolution electron microscopy (HREM) and crystallographic analysis (projection with different orientations by electron microscopy simulation). The principal twin structure in boron carbide particles is verified as (0001) twin, which can be attributed to $(01\bar{1}0)$ plane slip along the $1/3[\bar{1}100]$ direction, or the $(01\bar{1}0)$ plane slip along the $1/3[01\bar{1}0]$. In this case, the C–C–C chains experience slip along the characteristic slip system and, based on the displacement of C–C–C chains, the C–B bonds have corresponding rotation or reconfiguration due to geometric and electroneutrality constraints. Analysis of the loading conditions experienced by the boron carbide particles suggests that formation of the deformation twins is partly attributable to the presence of localized high stress and high shear force on the boron carbide particles during processing of the composite.

2. Experimental

The bulk nanostructured Al 5083/B_4C metal matrix composite was synthesized by cryomilling, degassing, cold isostatic pressing (CIP) and hot extrusion. Although additional details are reported elsewhere [5,18,19], a brief description is provided as follows. Particulate B_4C was blended with gas-atomized Al 5083 powder and then cryomilled in liquid nitrogen (89 K). The cryomilled composite powder was blended with additional unmilled Al 5083 powder and degassed. The degassed powder was cold isostatically pressed and then hot extruded at 798 K.

The TEM specimens were prepared by mechanically grinding the bulk materials to a thickness $<30\,\mu m$, then dimpling from both sides to a thickness of approximately $10\,\mu m$. Further thinning to a thickness of electron transparency was carried out using a Gatan PIPS 691 ion milling system at a voltage of 4 kV. A JEOL JEM 2500 SE transmission electron microscope operating at a voltage of 200 kV, equipped with Gatan imaging-filter (GIF) and energy dispersive X-ray spectroscopy (EDX) systems, was used for morphology images and high resolution transmission electron microscopy (HRTEM).

3. Result and discussion

In previous work [5], we report a super-high yield strength (up to 1065 MPa) for a nanostructured Al 5083/B_4C metal matrix composite consisting of micron-sized boron carbide reinforcement particles in a matrix with both coarse-grained (CG) and ultrafine-grained (UFG) Al 5083. The UFG Al grains ranged in size from ~30 to >300 nm; thus, the label of 'UFG' is more appropriate than 'nano-grained'. More specifically, the average grain size of the UFG Al is approximately 120 nm. In addition, there are two or three layers of UFG Al grains with an average grain size of 30–50 nm, which surround the boron carbide particles. Additional nanostructural features, such as intermetallic dispersoids, are also present, but a study of these features is beyond the scope of the current work. In the previous study, it was reported that UFG Al grains frequently surrounded the boron carbide particles and that the CG Al grains were randomly distributed throughout the matrix. Figure 1a shows a low magnification image of the nanostructured Al 5083/B_4C metal matrix composite, where four boron carbide particles are evident. All three boron carbide particles are surrounded by a region comprised of UFG Al grains and the size of the boron carbide particles range from 2 μm to approximately 500 nm. The average grain size of the UFG Al grains is approximately 120 nm and there are no coarse grains evident in this view. Figure 1b is the corresponding magnified image of particle "1" in Figure 1a; the thin clear twin plate is visible in the boron carbide particle. Additional defect structures also can be observed in the boron carbide particle (marked by white arrows). The high resolution TEM (HRTEM) image of the twin is shown in Figure 1c, obtained from the region enclosed by the rectangle in Figure 1b. It is evident that the width of the twin plates in the boron carbide particle is only ~6 nm, which is considerably thinner than twins found in metals. The corresponding fast Fourier transformation (FFT) pattern of the HRTEM image is shown in Figure 1d, in which the twin relationships are represented by two rectangles consisting of diffraction spots from twins and matrices. The twin plane is (0001) plane, which is the most common twin plane in the rhombohedral structure and consistent with the report of twins in boron carbide ceramic [16].

To provide insight into the structural details of twins in boron carbide particles, the local magnified HRTEM image of the twin in the boron carbide particle and its inverse FFT pattern were also acquired. As shown in Figure 2a, from the local magnified HRTEM image of the twin, the twin boundary is not straight and, moreover, there are ledges and irregularities in the region around the twin boundary (those marked by arrows). The obvious lattice mismatches in the center of the image

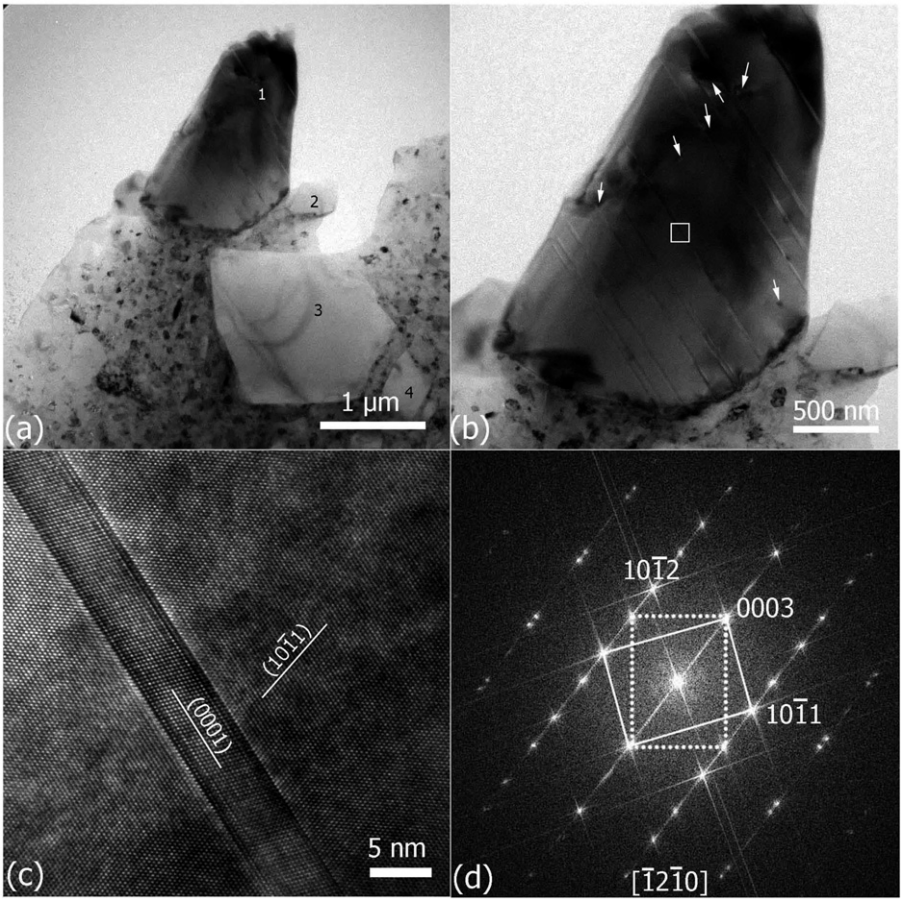

Figure 1. (a) Low magnification TEM image of a boron carbide particle and its ambient phase distribution. (b) Magnified TEM image of the boron carbide particle "1" in (a). (c) HRTEM image from the region enclosed by a rectangle in (b). (d) Corresponding FFT patterns of the HRTEM image in (b).

near the twin boundaries were marked by yellow lines. Most of the lattice mismatch disappeared in the lower part of the image (marked by another yellow line). Figure 2b is the corresponding inverse FFT pattern of Figure 2a (by selecting the (0003) and (000$\bar{3}$) diffraction spots from the FFT pattern), in which the dislocation structures show up clearly, and are marked by 'Ts' to indicate half an atomic plane. In addition, the curvature of the boron carbide lattice is also highlighted by ellipses. Figure 2c shows another HRTEM image of the twin with a relatively higher magnification, and its corresponding inverse FFT pattern (by selecting the (10$\bar{1}$1) and ($\bar{1}$01$\bar{1}$) diffraction spots of the matrix and twin from the FFT pattern) is shown in Figure 2d. We can see that there is obvious lattice mismatch at the twin boundaries; the typical lattice mismatch is highlighted by the red line. This behavior suggests displacement of the lattice plane (10$\bar{1}$1) along the [10$\bar{1}\bar{2}$] direction as in the case for Mg [20]. Typically a growth twin has perfect twin boundaries, which suggests that the observed 'jagged'

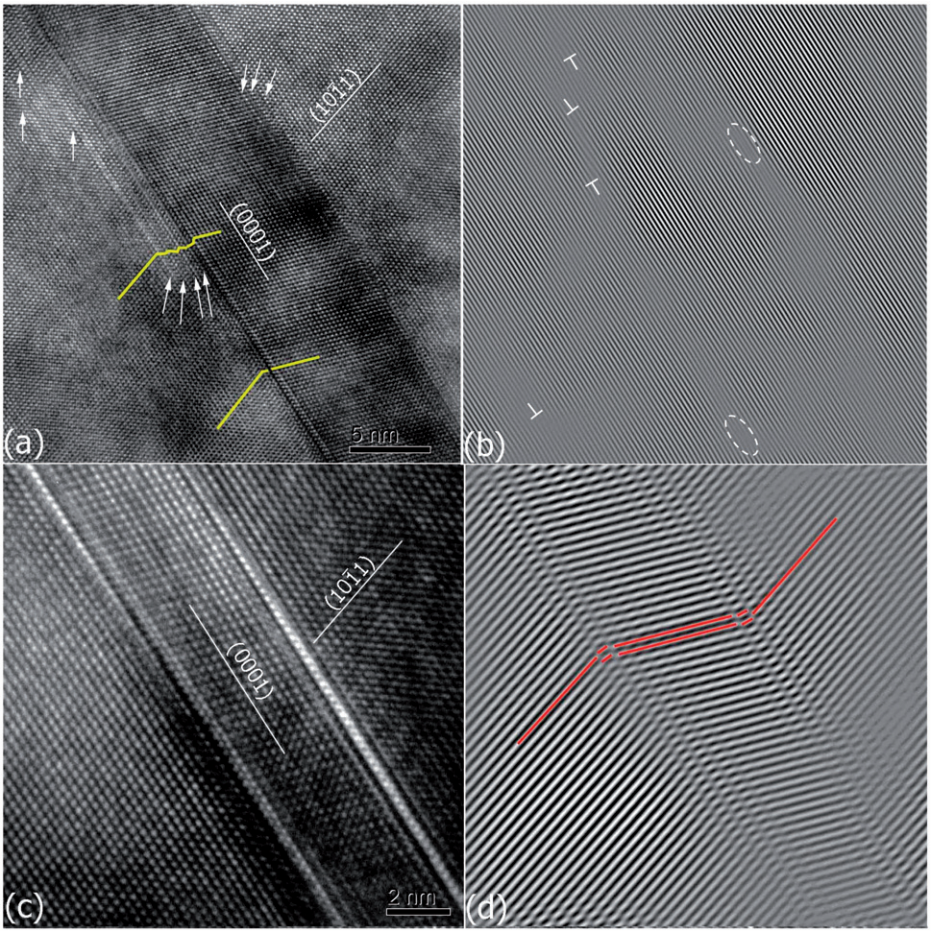

Figure 2. (a) Local magnified HRTEM image of the twin in the boron carbide particle and (b) its inverse FFT pattern, in which the dislocations are marked by 'T' and the curvature marked by ellipses. (c) Another HRTEM image showing the twin interface. (d) Corresponding FFT pattern of the image in (c).

twin boundaries are likely to contain defects. The twin morphology that is evident in Figure 1b suggests that the twin in the boron carbide particle is indeed a deformation twin, consistent with results reported by Ashbee [14].

To provide a fundamental insight into the mechanism(s) responsible for the formation of deformation twins in boron carbide, the crystal structure was simulated based on its crystallographic data. Figure 3a is a projection of the boron carbide crystal structure with the [$\bar{1}2\bar{1}0$] direction; the orange spheres represent the B atoms, and the gray ones represent the C atoms. The principal lattice planes (0001), (10$\bar{1}$1) and (10$\bar{1}$2) and lattice directions [0001] and [10$\bar{1}$0] are marked in the figure. Taking into account the crystallographic structure of boron carbide, the twin can form via two potential mechanisms: one involves a twin plane located in the region between two C–C–C chains (Figure 3b), whereas the second involves a twin plane passing

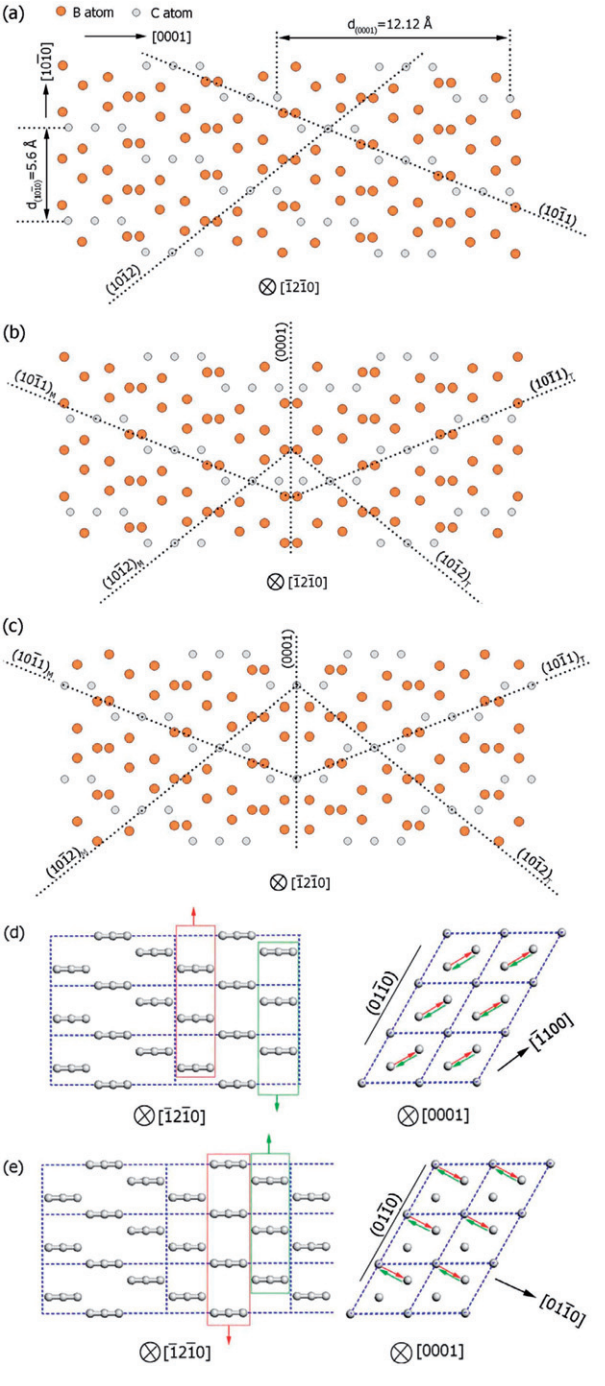

Figure 3. (a) Projection of the atomic structure of the [$\bar{1}$2$\bar{1}$0] direction of original boron carbide crystal; orange color = boron atoms; gray color = carbon. (b) and (c) Projections of the possible twin structures of boron carbide along the [$\bar{1}$2$\bar{1}$0] direction. (d) and (e) Potential formation model for the twin structures in (b) and (c).

through the C–C–C chains (Figure 3c). In Figure 3b, the projection shows that there are two C–C–C chains in the opposite position and it is noted that there is some distance between the two C–C–C chains due to the fact that they are not in the same plane. In the model shown in Figure 3c, the two C–C–C chains have a relatively longer distance than that corresponding to the model in Figure 3b, so this structure may be more reasonable for the twin in boron carbide. (Because the repulsive force between two C–C–C chains will induce the structure to become unstable, the longer distance between two C–C–C chains renders the model more stable.) To visualize the underlying mechanism, the B atoms were deleted from the boron carbide structure. As shown in Figure 3d, to form the twin in Figure 3b, the C–C–C chains within the red rectangle should slip 1/3 of a lattice distance in the upper direction and the C–C–C chains within the green rectangle should slip 1/3 of a lattice distance in the lower direction. The projection from the [0001] direction provides an illustration of this proposed mechanism. As shown in the figure, the atoms within the red rectangle have a slip $1/3[\bar{1}100]$ $(01\bar{1}0)$ and the alternative atoms within the green rectangle have a slip $1/3[1\bar{1}00]$ $(01\bar{1}0)$. For the model illustrated in Figure 3c, the movement of atoms is depicted in Figure 3e. The adjacent two group C–C–C chains slip with $1/3[01\bar{1}0]$ $(01\bar{1}0)$ (within the red rectangle) and $1/3[0\bar{1}10]$ $(01\bar{1}0)$ (within the green rectangle), respectively. This proposed model is consistent with the mechanism for twin formation in metals, in which partial dislocations $1/3$ $[01\bar{1}0]$ pass through the lattice along the slip direction [21,22]. The difference between metals and the mechanism proposed herein is that the displacements of the two rows of C–C–C chains in the unit cell slip along different directions in boron carbide. The B atoms around the C–C–C chains will slip together with the C–C–C chains, but this is not sufficient to account for twin formation. Therefore, the B–C bonds will experience rotations and distortions, and some B atoms will reconfigure their position to satisfy the requirement of electroneutrality and, hence, energy stability. Although additional studies are needed to confirm the basis of the mechanisms proposed herein, the proposed model provides an interesting fundamental insight into the phenomenon of twin formation in boron carbide.

Careful inspection of numerous boron carbide particles in the nanostructured Al 5083/B_4C metal matrix composite reveals that the presence of twins, while noted in some particles, was not prevalent. This suggests that there must have been local conditions responsible for the formation of twins in the boron carbide particles. The complexity of the synthesis steps used to prepare the composite (e.g. cryomilling, blending, degassing, cold isostatic pressing (CIP) and hot extrusion [5]) suggests that the local stress field experienced by the boron carbide particles is complex. However, detailed TEM characterization can provide fundamental insight into the conditions that promoted twin formation. As shown in the TEM image in Figure 4a, boron carbide particles containing twin structures were noted to be consistently surrounded by a layer of UFG Al grains (approximately 30–50 nm average grain size), with an additional two or three boron carbide particles in the vicinity. Figure 4b is a TEM image showing the interface between the boron carbide particles and the envelope of UFG Al grains. The presence of large curved contours indicates a very large extent of deformation around the boron carbide particle. A local magnified HRTEM image of Figure 4b (the area marked by a rectangle) is shown in Figure 4c, and its corresponding inverse FFT pattern (by selecting the $(1\bar{1}1)$ and $(\bar{1}1\bar{1})$ diffraction spots

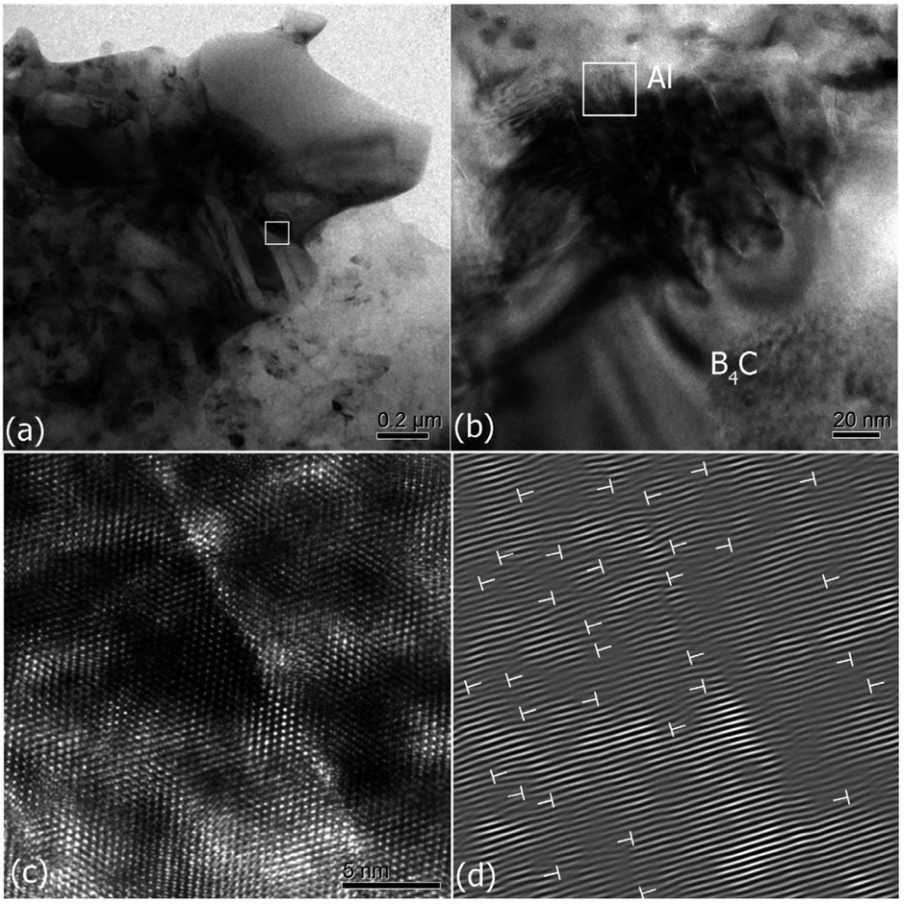

Figure 4. (a) Twinned boron carbide particle and its ambient phase distribution. (b) Low magnification TEM image of the interface between twinned boron carbide and surrounding UFG Al grains. (c) Local magnified HRTEM image from the region marked in (c). (d) Inverse FFT pattern of the image in (c), which shows the very high dislocation density around the twinned boron carbide particle.

of Al from the FFT pattern) is shown in Figure 4d. The dislocation structure is highlighted in Figure 4d, which shows a high dislocation density in the area surrounding the twinned boron carbide particle. The presence of a very high dislocation density supports the suggestion of a very high local stress on the twinned boron carbide particles, possibly exceeding the yield strength of boron carbide (e.g. 2.9 GPa). Careful study of additional interfaces between twinned boron carbide particles and the surrounding UFG Al grains revealed an interesting observation. At these interfaces, the twins ended or started at the side of twinned boron carbide particles, as illustrated in Figure 4b and are associated with a high dislocation density. In contrast, the interface between the UFG Al grains and the side of the boron carbide particle that is parallel to the twin plate reveals a low dislocation density. This observation suggests the presence of very high, non-isotropic local

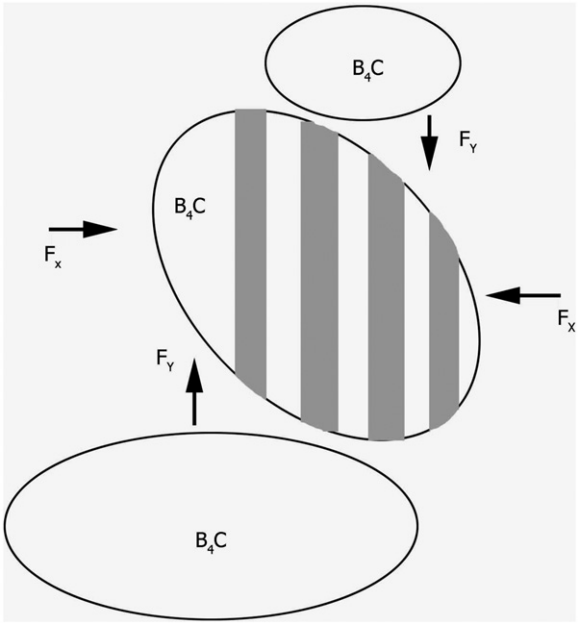

Figure 5. Schematic illustration of the loading conditions around the twinned boron carbide particle in the nanostructured Al 5083/B_4C metal matrix composite.

stresses around the twinned boron carbide particle. In this case, the stress parallel to the twin plates direction was probably higher than that perpendicular to the twin plates. Moreover, another experimental trend was noted through observation of a large number of boron carbide particles. As illustrated in the schematic diagram in Figure 5, near the twinned boron carbide particle, the other boron carbide particles in the vicinity are oriented perpendicular to the twin plates. In the positions that are parallel to the twin plates, however, UFG Al grains are observed (both Figures 1a and 4a demonstrate this). As a result, a local high shear force develops on the boron carbide particle $F_y > F_x$. Here, F_y is the force that is parallel to the twinning direction, whereas F_x is the force that is perpendicular to the twinning direction. The suggested presence of a high shear force field is consistent with the dislocation structure that was documented, and is also thought to be responsible for promoting deformation twins in the boron carbide particle. It is noted that the cryomilling may be another possible source of the twinning in the boron carbide particles. Thus far, however, twins have not been observed in the as-cryomilled powders, despite extensive TEM investigation. Continued investigation is ongoing and additional studies are underway to ascertain the validity of the mechanism suggested above.

4. Conclusions

The presence of deformation twins is documented in boron carbide reinforcement particles within a nanostructured Al 5083/B_4C metal matrix composite. The structure and formation mechanism of the twin was studied through detailed high resolution

transmission electron microscopy. Microstructure characterization shows that the principal twin structure in boron carbide particles is verified as (0001) twin, which can be attributed to $(01\bar{1}0)$ plane slip along the $1/3[\bar{1}100]$ direction, or the $(01\bar{1}0)$ plane slip along the $1/3[01\bar{1}0]$. Analysis of the loading conditions experienced by the boron carbide particles suggests that formation of the deformation twins is partly attributable to the presence of localized high stress and high shear force on the boron carbide particle, which occurs during processing.

Acknowledgement

The authors acknowledge financial support from Army Research Laboratory Cooperative Agreement No. W911NF-08-2-0028.

References

[1] C. Wood, D. Emin and P.E. Gray, Phys. Rev. B 31 (1985) p.6811.
[2] D. Emin, T.L. Aselage, A.C. Switendick, B. Morosin and C.L. Beckel, *Boron-Rich Solids*, AIP, New York, 1991.
[3] G.A. Samara, H.L. Tardy, E.L. Venturini, T.L. Aselage and D. Emin, Phys. Rev. B 48 (1993) p.1468.
[4] A.P. Newbery, S.R. Nutt and E.J. Lavernia, JOM. 58 (2006) p.56.
[5] J. Ye, B.Q. Han, Z. Lee, B. Ahn, S.R. Nutt and J.M. Schoenung, Scripta Mater. 53 (2005) p.481.
[6] J.F. Shackelford and W. Alexander, *CRC Materials Science and Engineering Handbook*, CRC Press LLC., Boca Raton, 2001.
[7] A.K. Bandyopadhyay, F. Beuneu, L. Zuppiroli and M. Beauvy, J. Phys. Chem. Solid. 45 (1984) p.207.
[8] B.J. Inkson, Acta Mater. 48 (2000) p.1883.
[9] A. Jostsons, C.K.H. Dubose, G.L. Copeland and J.O. Stiegler, J. Nucl. Mater. 49 (1973) p.136.
[10] S.L. Korinek and J. Castaing, J. Am. Ceram. Soc. 86 (2003) p.566.
[11] A.H. Heuer, K.P.D. Lagerlof and J. Castaing, Phil. Mag. A 78 (1998) p.747.
[12] W.F. Li, X.L. Ma, Y. Li, W.S. Zhang, W. Zhang and Z.D. Zhang, Phil. Mag. 85 (2005) p.3809.
[13] W.F. Li, X.L. Ma, Y. Li, W.S. Zhang and Z.D. Zhang, J. Mater. Res. 22 (2007) p.595.
[14] K.H.G. Ashbee, Acta Metall. 19 (1971) p.1079.
[15] K.H.G. Ashbee and C.K.H. Dubose, Acta Metall. 20 (1972) p.241.
[16] U. Anselmi-Tamburini, M. Ohyanagi and Z.A. Munir, Chem. Mater. 16 (2004) p.4347.
[17] I.D.R. Mackinnon, T. Aselage and S.B. Vandeusen, *American Instititute of Physics Conference Proceedings*, College Park, MD, 1986, p.114.
[18] J.C. Ye, J.H. He and J.M. Schoenung, Metall. Mater. Trans. A 37 (2006) p.3099.
[19] J.C. Ye, Z. Lee, B. Ahn, J.H. He, S.R. Nutt and J.M. Schoenung, Metall. Mater. Trans. A 37 (2006) p.3111.
[20] B. Li and E. Ma, Acta Mater. 57 (2009) p.1734.
[21] X.Z. Liao, F. Zhou, E.J. Lavernia, D.W. He and Y.T. Zhu, Appl. Phys. Lett. 83 (2003) p.5062.
[22] V. Yamakov, D. Wolf, S.R. Phillpot and H. Gleiter, Acta Mater. 50 (2002) p.5005.